Three-Dimensional Network-Structured Cyanide-Based Magnets

Joel S. Miller

Introduction

Magnets based on metal oxides have been important for hundreds of years. Magnetite, Fe_3O_4, Co-doped γ-Fe_2O_3, and CrO_2 are important examples. The oxide (O^{2-}) bridge between the magnetic metal ions has filled *p* orbitals (Figure 1a) that provide the pathway for strong spin coupling. Albeit with twice as many atoms, cyanide ($C{\equiv}N^-$) can bridge between two metal ions via its pair of empty antibonding orbitals (Figure 1b) and filled nonbonding orbitals. Even prior to a detailed understanding of either their composition or structure, magnetic ordering of several cyanide complexes, although at low temperature, was noted.[1] The differing atoms at each end of the cyanide ion have different binding affinities to metal ions, and simple coordination compounds, for example, $[Fe^{II}(CN)_6]^{2-}$ (ferrocyanide), with alkali cations can easily be made. Replacement of the alkali cations with transition-metal cations affords insoluble materials, for example $Fe^{III}_4[Fe^{II}(CN)_6]_3$ (Prussian blue). Prussian blue has been used as a pigment and as an electrochromic and electrocatalyst material.[2] The structure of Prussian blue was elucidated[3] to be cubic (isotropic) with $\rightarrow Fe^{II}\leftarrow C{\equiv}N\rightarrow Fe^{III}\leftarrow N{\equiv}C\rightarrow Fe^{II}\leftarrow$ linkages along all three crystallographic directions (Figure 2). The $Fe^{II}\cdots Fe^{III}$ separation is ~5 Å. However, based on the composition, this is an idealized structure, as one Fe^{II} site per unit cell is missing. Water fills the vacant sites as well as the channels present in the structure. Due to the structural defects, it has been a challenge to grow single crystals.

The metal ion, its oxidation state, and, consequently, its number of spins per site can be altered with relative ease, leading to a variety of magnetic behaviors.[4] Depending on the charges, the modified Prussian

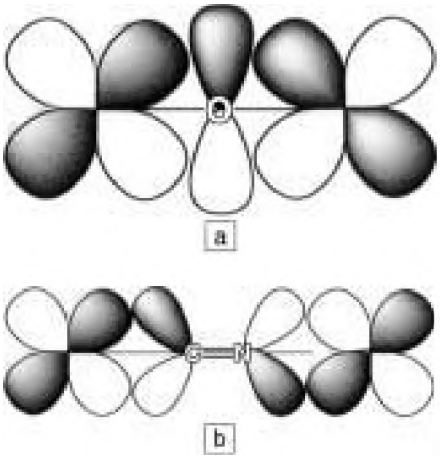

Figure 1. Orbital overlap diagram for (a) an M–O–M bridge with filled oxygen p orbitals and for (b) an M–CN–M bridge with empty π orbitals.

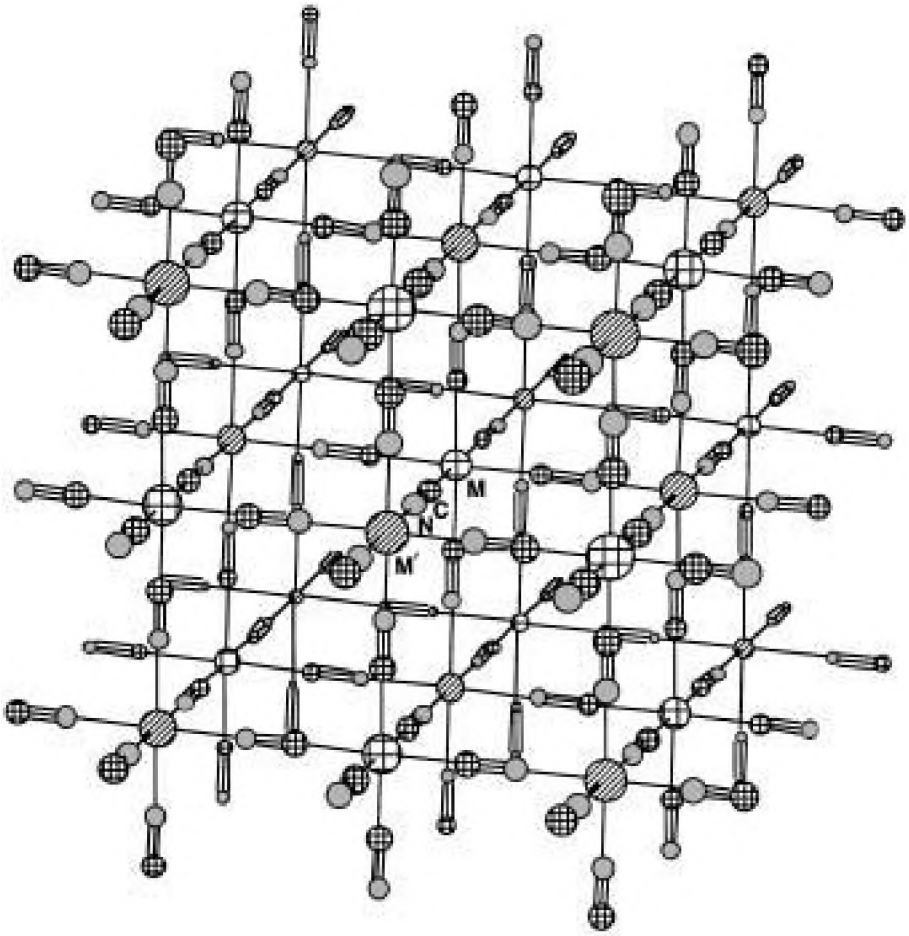

Figure 2. Idealized structure of Prussian blue type material with $\rightarrow M'\leftarrow C{\equiv}N\rightarrow M\leftarrow C{\equiv}N\rightarrow M'\leftarrow$ linkages along all three crystallographic directions. For Prussian blue, M = Fe^{II} and M′ = Fe^{III}.

blue may have more or fewer structural defects. For example, $Ni^{II}_3[Cr^{III}(CN)_6]_2$ has 4/3 $[Cr^{III}(CN)_6]^{3-}$ sites per unit cell missing and filled with water, while $CsNi^{II}[Cr^{III}(CN)_6]$ has no defects in the metal-ion sites, but has an interstitial Cs^+ ion.

Neglecting defects, the Prussian blue structure type is composed of $M'_y[M(CN)_6]$, with M always being C-bound and M′ being N-bound. Due to the strong ligand field character of the cyanide ligand, the C-bound M is always low spin. In contrast, the N-bound M′ is high spin. Thus, for $Fe^{III}_4[Fe^{II}(CN)_6]_3$, the d^6 Fe^{II}'s are low spin ($S = 0$) (Figure 3a), while the d^5 Fe^{III}'s are high spin ($S = 5/2$) (Figure 3b). Consequently, the only spin coupling is between distant Fe^{III} sites. Nonetheless, ferromagnetic ordering occurs at 5.6 K.[3]

Both ferro- and antiferromagnetic coupling leading to ferro- or ferrimagnetic ordering can occur and can be predictably controlled. The type of ordering can be reliably predicted from a consideration of the orbitals in which the spins reside on adjacent M and M′ sites. Ferromagnetic coupling occurs when spins on nearest-neighbor metal-ion sites are in orthogonal orbitals. From ligand field theory, the $d_{x^2-y^2}$ and d_{z^2} orbitals are orthogonal to the lower-energy d_{xy}, d_{xz}, and d_{yz} orbitals. Thus, this occurs for d^8 Ni^{II} ($d_{x^2-y^2}{}^1$, $d_{z^2}{}^1$) and d^3 Cr^{III} ($d_{xy}{}^1$, $d_{xz}{}^1$, $d_{yz}{}^1$) metal ions as $Ni^{II}_3[Cr^{III}(CN)_6]_2\cdot xH_2O$ orders ferromagnetically below a T_c of 72 K.[5] In contrast, when the spin-containing orbitals are not orthogonal, the unpaired spins couple antiferromagnetically, leading to a ferrimagnet. This is observed for d^5 Mn^{II} ($d_{x^2-y^2}{}^1$, $d_{z^2}{}^1$, $d_{xy}{}^1$, $d_{xz}{}^1$, $d_{yz}{}^1$) and d^3 Cr^{III} in $Mn^{II}_3[Cr^{III}(CN)_6]_2\cdot xH_2O$ (T_c = 67 K),[5] which order ferrimagnetically. Many magnets complying with this paradigm have been reported[4,5] (See Table I).

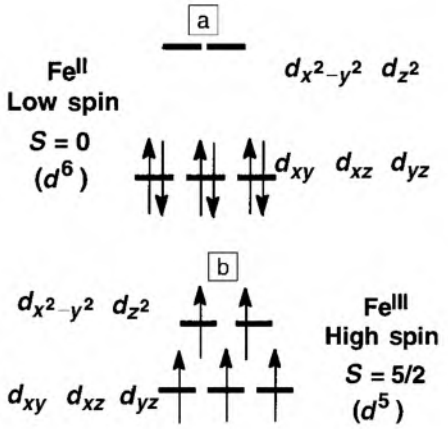

Figure 3. Crystal field diagram for the 3d orbitals on (a) low-spin Fe^{II} and (b) high-spin Fe^{III}.

Table I: Representative Prussian Blue Structured Magnets and Their Critical Temperatures (T_c)

Composition	T_c (K)	Ordering[a]	Reference
$Fe^{III}_4[Fe^{II}(CN)_6]_3\cdot xH_2O$, Prussian blue	5.6[b]	FO	3
$CsNi^{II}[Cr^{III}(CN)_6]\cdot 2H_2O$	90	FO	4
$Ni^{II}_3[Cr^{III}(CN)_6]_2\cdot xH_2O$	72	FO	5
$CsMn^{II}[Cr^{III}(CN)_6]\cdot H_2O$	90	FI	4
$Mn^{II}_3[Cr^{III}(CN)_6]_2\cdot xH_2O$	67	FI	5
$Cr^{III}\{[Cr^{III}(CN)_6]_{0.98}[Cr^{II}(CN)_6]_{0.02}\}$	230[b]	FI	12
$K_{2.0}Cr^{II}[Cr^{II}(CN)_6]$	135[b]	FI	12
$V^{II}_{0.42}V^{III}_{0.58}[Cr^{III}(CN)_6]_{0.86}\cdot 2.8H_2O$	315	FI	6
$Cr^{III}[Cr^{III}(CN)_6]_{0.95}[Cr^{II}(CN)_6]_{0.05}$	260[b]	FI	12
$K_{0.058}V^{II}_{0.57}V^{III}_{0.43}[Cr^{III}(CN)_6]_{0.79}(SO_4)_{0.058}\cdot 0.93H_2O$	372	FI	7
$KV^{II}[Cr^{III}(CN)_6]\cdot 2H_2O\cdot 0.1K[O_3SCF_3]$	376	FI	8

[a] FO = ferromagnet, FI = ferrimagnet.
[b] Thin films have been prepared electrochemically.

Room-Temperature Magnets

Through numerous years of study, many magnets based on Prussian blue have been reported. Those with M′ = Ni and Cu order ferromagnetically, while the others order as ferrimagnets. Ferrimagnets with lower-saturation magnetizations than ferromagnets frequently have the higher ordering temperatures. Use of M′ = V^{II} and M = Cr^{III} has led to the discovery of Prussian blue structured magnets that order above room temperature. $V^{II}_{0.42}V^{III}_{0.58}[Cr^{III}(CN)_6]_{0.86}\cdot 2.8H_2O$ ordered as a ferrimagnet above room temperature at 315 K.[6] Air oxidation, however, leads to $(V^{IV}O)[Cr^{III}(CN)_6]_{0.67}\cdot 3.33H_2O$, with its ordering temperature reduced to 115 K.[6] Later, a more complex formulation was reported to order at 372 K.[7] Although it is compositionally more complex, the 372 K magnet (Figure 4) has enhanced stability even upon exposure to air (Figure 5). Simultaneously, a related, formally stoichiometric magnet was reported by Holmes and Girolami.[8]

Figure 4. Photograph of a polycrystalline sample of nominally $K_{0.058}V^{II/III}[Cr^{III}(CN)_6]_{0.79}\cdot(SO_4)_{0.058}\cdot 0.93H_2O$ being attracted to a Teflon-covered magnet in air at room temperature. Copyright 1999 J.S. Miller.

Controlling Properties by Means of Solid Solutions

Specific magnetic properties and combinations with other physical properties can be achieved using solid solutions of Prussian blue structured magnets. Depending on x, solid solutions of $Mn^{II}_{3-x}Ni^{II}_x[Cr^{III}(CN)_6]_2\cdot yH_2O$ can exhibit ferro- ($x < 0.5$) or ferrimagnetic ($x > 0.5$) behavior,[5] and the saturation magnetization varies with x (Figure 6). The structure of the solid solutions is that depicted in Figure 2, with Mn^{II} and Ni^{II} randomly occupying the M′ sites. Since the ferromagnetic Ni^{II}/Cr^{III} (T_c = 72 K) and ferrimagnetic Mn^{II}/Cr^{III} (T_c = 67 K) sublattices have different temperature dependencies of the magnetization, $M(T)$, the net magnetization due to their relative ratio can be dramatically different, and all four types of $M(T)$'s—the behaviors theoretically predicted by Néel, including one with a double maxima and a compensation temperature [T at which $M(T) = 0$]—are observed[5] (Figure 7).

Likewise, the coercive field H_{cr} can be controlled (Figure 6). In contrast, solid solutions of $Cr^{II}_{3-x}Fe^{II}_x[Cr^{III}(CN)_6]_2\cdot yH_2O$

composition can be used to control the color of the magnet in addition to the magnetic behavior (Figure 6). Colorless magnets occur for $x = 0$, while $x = 0.2$ gives violet, $x = 0.4$ gives red, and $x = 1$ gives orange magnets.[9]

More complex ternary solid solutions can lead to more complex but controlled magnetic behavior. Solid solutions of $Mn^{II}_aFe^{II}_bNi^{II}_c[Cr^{III}CN)_6]_2 \cdot xH_2O$ ($a + b + c = 3$) possess three sublattices: ferrimagnetic Mn^{II}/Cr^{III} ($T_c = 67$ K) and Fe^{II}/Cr^{III} ($T_c = 27$ K) sublattices and a ferromagnetic Ni^{II}/Cr^{III} ($T_c = 72$ K) sublattice.[10] The structure of this ternary solid solution is that depicted in Figure 2, except that Fe^{II}, Mn^{II}, and Ni^{II} randomly occupy the M′ sites. Note that the metal ions represent four different spin centers, namely, $S = 1$ (Ni^{II}), $S = 3/2$ (Cr^{III}), $S = 2$ (Fe^{II}), and $S = 5/2$ (Mn^{II}). The material with the composition $Mn^{II}_{1.80}Fe^{II}_{0.54}Ni^{II}_{0.66}[Cr^{III}(CN_6]_2 \cdot 15.2H_2O$ orders at 62 K, and due to the competition between the several sublattices, it exhibits two compensation temperatures (35 K and 53 K)[10] (Figure 8).

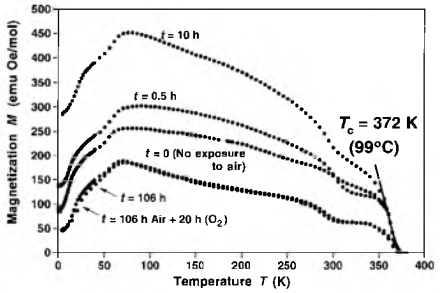

Figure 5. Temperature-dependence of the magnetization of nominally $K_{0.058}V^{II/III}[Cr^{III}(CN)_6]_{0.79} \cdot (SO_4)_{0.058} \cdot 0.93H_2O$ upon exposure to air and pure oxygen for up to 106 h for air and an additional 20 h of O_2. Note that the 372 K T_c is not altered.

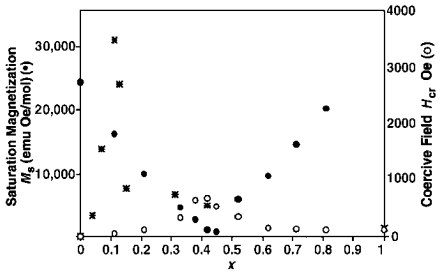

Figure 6. Saturation magnetization M_s (●) and coercive field H_{cr} (○) as a function of x for $Mn^{II}_{3-x}Ni^{II}_x[Cr^{III}(CN)_6]_2 \cdot yH_2O$, and H_{cr} as a function of x for $Fe^{II}_xMn^{II}_{3-x}[Cr^{III}(CN)_6]_2 \cdot yH_2O$ (■).

Thin-Film Magnets

Magnetic thin films are technologically important. Expanding upon work using Prussian blues as electrochromic materials,[2] films based on $[Cr^{III}(CN)_6]^{3-}$ have been electrochemically deposited onto indium-doped tin oxide (ITO)[11,12] and glassy carbon electrodes.[12] Depending on the electrochemical conditions, either oxidized or reduced, amorphous (Figure 9a) or crystalline (Figure 9b) films (1.0 ± 0.5 μm) can be electrodeposited.[12] The oxidized and reduced films have compositions of $Cr^{III}\{[Cr^{III}(CN)_6]_{0.98}[Cr^{II}(CN)_6]_{0.02}\}$ and $K_{2.0}Cr^{II}[Cr^{II}(CN)_6]$, respectively. T_c varies with the degree of oxidation and ranges between 135 K for the reduced films and 260 K for the oxidized films, independent of crystallinity. Hysteresis with coercive fields as high as 830 Oe at 20 K is observed for the amorphous material and is substantially less for the crystalline material. This is ascribed to the greater number of defects in the amorphous films. Upon electrochemical oxidation of the films the magnetic behavior is altered such that, for example, at 150 K the film becomes ferromagnetic[11] (Figure 10).

The *M(T)* data also reveal "freezing-in" or negative magnetization upon cooling to 20 K in a negative applied dc field. The *M(T)*'s obtained on cooling in opposite fields of equal strength are nearly symmetric about the zero-field-cooled (ZFC) magnetization (Figure 11). ZFC measurements result in a positive magnetization reduced by more than an order of magnitude from field-cooled (FC) data, but both the ZFC and FC magnetization data converge to the same T_c. This negative (re-

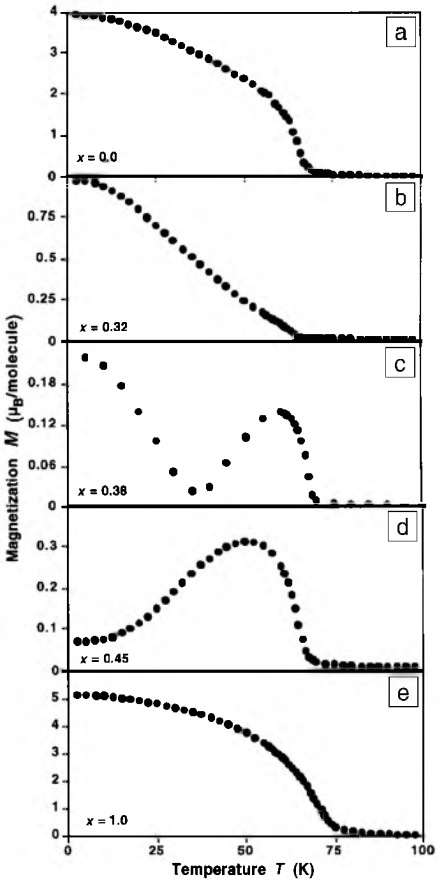

Figure 7. Temperature-dependencies of the magnetization for $Mn^{II}_{3-x}Ni^{II}_x[Cr^{III}(CN)_6]_2 \cdot yH_2O$ as a function of x; (a) x = 0, (b) x = 0.32, (c) x = 0.38, (d) x = 0.45, and (e) x = 1.

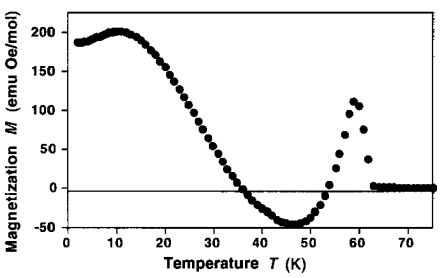

Figure 8. Temperature-dependencies of the magnetization for $Mn^{II}_{1.80}Fe^{II}_{0.54}Ni^{II}_{0.66}[Cr^{III}(CN)_6]_2 \cdot 15.2H_2O$, revealing compensation temperatures at 35 K and 53 K.

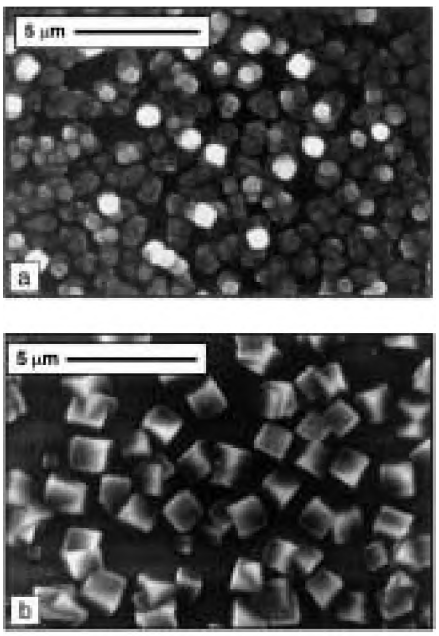

Figure 9. Scanning electron microscopy images of (a) an amorphous film and (b) a crystalline film.

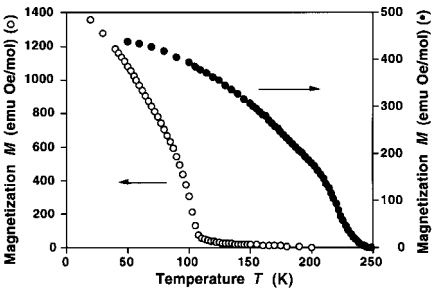

Figure 10. Change in the magnetic behavior of $Cr^{II}_{1.14}Cr^{II}_{1.29}[Cr^{II}(CN)_6]\cdot 6.09H_2O$ upon changing the electrochemical potential. (From Reference 11.)

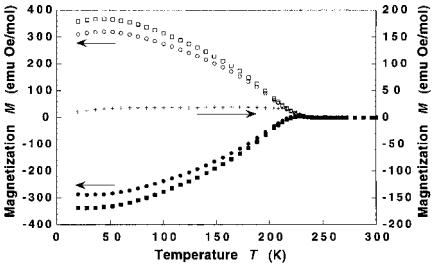

Figure 11. Temperature-dependent magnetization of an amorphous $Cr^{III}\{[Cr^{III}(CN)_6]_{0.98}[Cr^{II}(CN)_6]_{0.02}\}$ film, zero-field-cooled (+) and field-cooled in 5 Oe (○), −5 Oe (●), 10 Oe (□), and −10 Oe (■).

versed) magnetization is observed in all $K_nCr_x[Cr(CN)_6]$ films studied. Fields as high as about 100 Oe are necessary, at 20 K, to reverse the negative magnetization for samples cooled in −5 Oe.[12]

Thin films of the room-temperature $V^{II}[Cr(CN)_6]$ magnet, as well as more complex compositions,[4] have also been prepared. Thin films (ca. 2 μm) composed of a solid solution of $Cr^{II}_{3-x}Fe^{II}_x[Cr^{III}(CN)_6]_2\cdot xH_2O$, where x and the film color can be controlled by the electrochemical potential, have been prepared electrochemically.[9]

Photomagnetic Behavior

Altering the magnetic behavior with incident light, especially to an ordered magnetic state, is an important area of contemporary research. This effect has been reported for electrochemically deposited thin films (0.05–1.0 μm) of $K_{0.4}Co_{1.3}[Fe(CN)_6]\cdot 5H_2O$.[13] Upon illumination with visible light, paramagnetic $K_{0.4}Co_{1.3}[Fe(CN)_6]\cdot 5H_2O$ orders magnetically at 26 K (Figure 12). Detailed study of this reaction has led to the characterization of $K_{0.4}Co_{1.3}[Fe(CN)_6]$ as containing mixed-valent Co, that is, $K_{0.4}Co^{II}_{0.3}Co^{III}[Fe^{II}(CN)_6]$ N-bound. Here, anomalously, low-spin Co^{III}, as well as high-spin Co^{II}, is N-bound to the cyanide. The nonstoichiometry suggests a defect-ridden structure. The onset of magnetic ordering is attributed to photoinduced electron transfer:

$$(S_{Fe^{II}} = 0)\ Fe^{II}\leftarrow C\equiv N\rightarrow Co^{III}\ (S_{Co^{III}} = 0)$$
$$\longrightarrow (S_{Fe^{III}} = 1/2)\ Fe^{III}\leftarrow C\equiv N\rightarrow Co^{II}\ (S_{Co^{II}} = 3/2); \quad (1)$$

thus, diamagnetic $Fe^{II}\leftarrow C\equiv N\rightarrow Co^{III}$ ($S_{total} = 0 + 0 = 0$) becomes paramagnetic ($S_{total} = 3/2 - 1/2 = 1$) and can couple other spins in the solid, leading to an ordered magnetic state. This state is reversible upon illumination with near-infrared light. The magnetization can be further enhanced by 20% upon application of a 5-T applied magnetic field.[13] In a related system, the photoinduced magnetism is attributed to cluster glass formation.[14]

Through the judicial choice of the composition of a Prussian blue structured magnet, the direction of magnetization can be induced to switch upon illumination. This phenomenon is used in magneto-optical memories. In accord with other Prussian blue structured solid solutions, $Fe^{II}_{1.20}Mn^{II}_{1.80}[Cr^{III}(CN)_6]_2\cdot 15H_2O$ exhibits a compensation temperature of 19 K for magnetization taken in a 10-Oe applied field[15] (Figure 13). Illumination with 360–450-nm light at 16 K led to the magnetization increasing to a positive value, and this state persisted for several days. Hence, the direction of magnetization can be reversed by light.

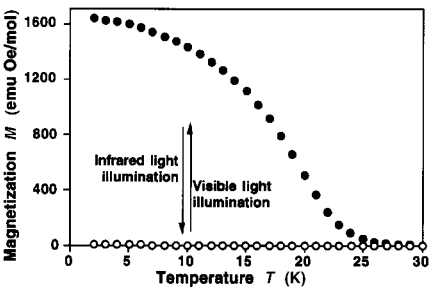

Figure 12. Change in the magnetization of $K_{0.4}Co_{1.3}[Fe(CN)_6]\cdot 5H_2O$ from the paramagnetic state to a magnetically ordered state upon illumination with visible light and reversal upon illumination with near-infrared light.

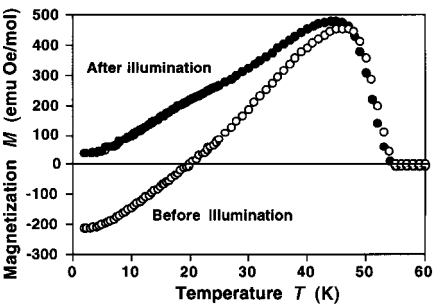

Figure 13. Illumination with 360–450 nm light of $Fe^{II}_{1.20}Mn^{III}_{1.80}[Cr^{III}(CN)_6]_2\cdot 15H_2O$, increasing the magnetization to a positive value from a negative value.

Extensions from Prussian Blue Structured Magnets

The success in preparing magnets based upon the Prussian blue structure has led to studies of other percyanometal complexes. In addition to hexacoordinate complexes, paramagnet building blocks of $[M(CN)_x]^{z-}$ (x = 4, 5, 7, and 8) are known, and several materials of $M'_y[M(CN)_x]$ composition have been reported to magnetically order. For example, $Mn^{II}_2(OH_2)_5[Mo^{III}(CN)_7]\cdot xH_2O$ forms several phases that order as ferromagnets at 51 K, while $K_2Mn^{II}_3(OH_2)_6[Mo^{III}(CN)_7]_2\cdot xH_2O$ orders as a ferromagnet at 39 K.[16] Due to the heptacoordination about the Mo^{III} site, noncubic anisotropic three-dimensional and two-dimensional structures are observed, respectively. Dehydration of $K_2Mn^{II}_3(OH_2)_6[Mo^{III}(CN)_7]_2\cdot xH_2O$ enhances the T_c to 72 K. A key feature of this material is that it orders as a ferromagnet, which is not understood.[16] Additionally, $Cu^{II}_3[W^{V}(CN)_8]_2\cdot 3.4H_2O$, which magnetically orders at 50 K, has been prepared.[17]

Magnetic ordering has also been observed for pentacyano octahedral metal complexes, $[M(CN)_5X]^{z-}$ (X = NO, N). The structure of $M'[M(CN)_5X]$ is that shown in Figure 2, with one cyanide per M randomly replaced by either NO or N. Both $Cr_2[Cr(CN)_5NO]\cdot 4H_2O\cdot 3.6MeOH$ (Reference 18) and $Cr[Cr(CN)_4N]\cdot x$MeOH (Reference 19) are magnets below 127 K and 151 K, respectively. Photomagnetic behavior is also observed in the related $Ni^{II}[Fe^{II}(CN)_5NO]\cdot 5.3H_2O$.[20]

Conclusions

Materials of $M'_y[M(CN)_6]$ composition possessing the Prussian blue structure, due to the bridging of the metal sites with the conjugated cyanide ligand, exhibit strong magnetic coupling and magnetic ordering. Both ferromagnetic and ferrimagnetic behavior has been observed. Magnets with critical temperatures exceeding room temperature have been made, and both binary and ternary solid solutions with unusual but predictable properties

can be made. The T_c, saturation magnetization, and coercive fields, as well as color in some cases, can be controlled. Thin-film magnets can be electrochemically fabricated, and their magnetic properties and, in some cases, their color can be controlled by the electrochemical potential. The magnetic behavior can also be controlled, even reversibly, with light, and in some cases, the direction of magnetization can be reversed by illumination. The breadth and diversity of physical properties of this class of magnets make them strong candidates for technological development.

Acknowledgments

The author gratefully acknowledges the invaluable support that numerous collaborators have made over the years. Special thanks are extended to Prof. Gregory S. Girolami (University of Illinois) and Prof. Michel Verdaguer (Université Pierre et Marie Curie) for enabling me to write this review. The author also thanks the U.S. Department of Energy (grant Nos. DE-FG03-93ER45504 and DE-FG02-96ER12198) and the Air Force Office of Scientific Research (grant No. F49620-00-1-0055) for their support.

References

1. R.M. Bozorth, H.J. Williams, and D.E. Walsh, *Phys. Rev.* **103** (1956) p. 572; A.N. Holden, B.T. Matthias, P.W. Anderson, and H.W. Lewis, *Phys. Rev.* **102** (1956) p. 1463.
2. K. Itaya, I. Uchida, and V.D. Neff, *Acc. Chem. Res.* **19** (1986) p. 162.
3. F. Herren, P. Fischer, A. Ludi, and W. Hälg, *Inorg. Chem.* **19** (1980) p. 956.
4. M. Verdaguer, A. Bluezen, C. Train, R. Garde, F. Fabrizi de Biani, and C. Desplanches, *Philos. Trans. Soc. London, Ser. A* **357** (1999) p. 2959; M. Verdaguer, A. Bluezen, V. Marvaud, J. Waissermann, M. Seuleimann, C. Desplanches, A. Scuiller, C. Train, R. Garde, G. Gelly, C. Lomenech, I. Rosenman, P. Veillet, C. Cartier, and F. Villain, *Coord. Chem. Rev.* **190–192** (1999) p. 1023; W.R. Entley, C.R. Treadway, and G.S. Girolami, *Mol. Cryst. Liq. Cryst.* **273** (1995) p. 153.
5. S. Ohkoshi, T. Iyoda, A. Fujishima, and K. Hashimoto, *Phys. Rev.* **56** (1997) p. 11642.
6. S. Ferlay, T. Mallah, R. Ouahes, P. Veillet, and M. Verdaguer, *Nature* **378** (1995) p. 701; E. Dujardin, S. Ferlay, X. Phan, C. Desplanches, C.C.D. Moulin, P. Sainctavit, F. Baudelet, E. Dartyge, P. Veillet, and M. Verdaguer, *J. Am. Chem. Soc.* **120** (1998) p. 11347; S. Ferlay, T. Mallah, R. Ouahes, P. Veillet, and M. Verdaguer, *Inorg. Chem.* **38** (1999) p. 229.
7. Ø. Hatlevik, W.E. Buschmann, J. Zhang, J.L. Manson, and J.S. Miller, *Adv. Mater.* **11** (1999) p. 914.
8. S.D. Holmes and G.S. Girolami, *J. Am. Chem. Soc.* **121** (1999) p. 5593.
9. S. Ohkoshi, A. Fujishima, and K. Hashimoto, *J. Am. Chem. Soc.* **120** (1998) p. 5349.
10. S. Ohkoshi, Y. Abe, A. Fujishima, and K. Hashimoto, *Phys. Rev. Lett.* **82** (1999) p. 1285.
11. O. Sato, T. Iyoda, A. Fujishima, and K. Hashimoto, *Science* **271** (1996) p. 49.
12. W.E. Buschmann, S.C. Paulson, C.M. Wynn, M. Girtu, A.J. Epstein, H.S. White, and J.S. Miller, *Chem. Mater.* **10** (1998) p. 1386.
13. O. Sato, Y. Einaga, T. Iyoda, A. Fujishima, and K. Hashimoto, *J. Electrochem. Soc.* **144** (1997) p. L11; Y. Einaga, O. Sato, S. Ohkoshi, A. Fujishima, and K. Hashimoto, *Chem. Lett.* (1998) p. 585.
14. D.A. Pejakovic, J.L. Manson, J.S. Miller, and A.J. Epstein, *J. Appl. Phys.* **87** (2000) p. 6028.
15. S. Ohkoshi and K. Hashimoto, *J. Am. Chem. Soc.* **121** (1999) p. 10591.
16. O. Kahn, J. Laorionova, and L. Ouahab, *Chem. Commun.* (1999) p. 945.
17. R. Garde, C. Desplanches, A. Bluezen, P. Veillet, and M. Verdaguer, *Mol. Cryst. Liq. Cryst.* **334** (1999) p. 587.
18. S.D. Holmes and G.S. Girolami, *Mol. Cryst. Liq. Cryst.* **305** (1997) p. 287.
19. S.R. Marshall, J. Bendix, and J.S. Miller (unpublished).
20. Z.-Z. Gu, O. Sato, T. Iyoda, K. Hashimoto, and A. Fujishima, *Chem. Mater.* **9** (1997) p. 1092.

■